Journal of Advanced Research 38 (2022) 179–190

Contents lists available at ScienceDirect

Journal of Advanced Research

journal homepage: www.elsevier.com/locate/jare

Exact analysis and elastic interaction of multi-soliton for a two-dimensional Gross-Pitaevskii equation in the Bose-Einstein condensation

Haotian Wang [a], Qin Zhou [b,c], Wenjun Liu [a,*]

[a] State Key Laboratory of Information Photonics and Optical Communications, and School of Science, Beijing University of Posts and Telecommunications, P. O. Box 122, Beijing 100876, China
[b] School of Mathematics and Physics, Hubei Polytechnic University, Huangshi 435003, China
[c] Nonlinear Analysis and Applied Mathematics (NAAM)-Research Group, Department of Mathematics, Faculty of Science, King Abdulaziz University, P.O. Box 80257, Jeddah 21589, Saudi Arabia

HIGHLIGHTS

- We investigated a two-dimensional Gross-Pitaevskii equation with time-varying trapping potential in the Bose-Einstein condensation.
- The Hirota bilinear method is established to solve the two-dimensional Gross-Pitaevskii equation and its parabolic soliton, line-soliton and dromion-like structure can be exhibited via some appropriate parameters chosen. Their interaction structures are discussed.
- The interaction of two-soliton solutions is investigated through asymptotic analysis.

GRAPHICAL ABSTRACT

Interaction of two solitons with different structures is exhibited. By adjusting the corresponding parameters, distinct solitons and their interaction can be achieved. It can also simulate a process of energy concentration of solitons at different times.

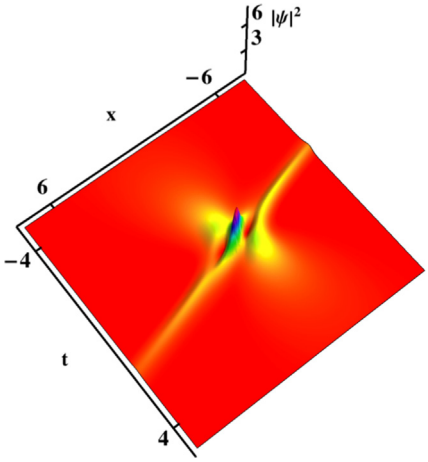

ARTICLE INFO

Article history:
Received 12 July 2021
Revised 15 September 2021
Accepted 16 September 2021
Available online 20 September 2021

Keywords:
Two-dimensional Gross-Pitaevskii equation
Hirota bilinear method

ABSTRACT

Introduction: The Gross-Pitaevskii equation is a class of the nonlinear Schrödinger equation, whose exact solution, especially soliton solution, is proposed for understanding and studying Bose-Einstein condensate and some nonlinear phenomena occurring in the intersection field of Bose-Einstein condensate with some other fields. It is an important subject to investigate their exact solutions.
Objectives: We give multi-soliton of a two-dimensional Gross-Pitaevskii system which contains the time-varying trapping potential with a few interactions of multi-soliton. Through analytical and graphical analysis, we obtain one-, two- and three-soliton which are affected by the strength of atomic interaction. The asymptotic expression of two-soliton embodies the properties of solitons. We can give some

Peer review under responsibility of Cairo University.
* Corresponding author.
E-mail address: jungliu@bupt.edu.cn (W. Liu).

https://doi.org/10.1016/j.jare.2021.09.007

Exact bright soliton solutions
Multi-soliton interactions
Asymptotic analysis
Bose-Einstein condensation

interactions of solitons of different structures including parabolic soliton, line-soliton and dromion-like structure.
Methods: By constructing an appropriate Hirota bilinear form, the multi-soliton solution of the system is obtained. The soliton elastic interaction is analyzed via asymptotic analysis.
Results: The results in this paper theoretically provide the analytical bright soliton solution in the two-dimensional Bose-Einstein condensation model and their interesting interaction. To our best knowledge, the discussion and results in this work are new and important in different fields.
Conclusions: The study enriches the existing nonlinear phenomena of the Gross-Pitaevskii model in Bose-Einstein condensation, and prove that the Hirota bilinear method and asymptotic analysis method are powerful and effective techniques in physical sciences and engineering for analyzing nonlinear mathematical-physical equations and their solutions. These provide a valuable basis and reference for the controllability of bright soliton phenomenon in experiments for high-dimensional Bose-Einstein condensation.

Introduction

Some specific nonlinear wave models, e.g. soliton, is a common localized wave and arises from the balance between nonlinear and dispersive effects [1]. Solitary waves are largely put to use to understand and describe various phenomena in science and engineering fields such as Bose-Einstein condensate (BEC) [2,3,4], plasma physics [5], hydrodynamics [5,6], fluid mechanics [7] and nonlinear optics [8,9,10,11,12]. In particular, the study and development of optics including pulsed fiber lasers [8], optical communications [9,10], all-optical switches [11] and nonlinear fibers [12] depend on research of novel multi-soliton interaction phenomena. Nowadays, the search for soliton solutions of nonlinear equations takes a leading contribution in mathematics and physics. Therefore, some effective and capable methods have been established for attaining the soliton solutions of nonlinear equations in the years past, such as, Hirota bilinear method, Darboux transformation, inverse scattering transforms, the extended tanh-function scheme, $\exp_a$-function, unified methods, generalized exponential rational function method, (G'/G)-expansion method, the function ansatz method, trial function method, improved $\tan(\phi(\eta)/2)$-expansion method, Lie symmetry method, generalized Kudryashov method, sine-Gordon expansion approach, modified auxiliary expansion method, Bernoulli sub-equation function method and so forth [13–22]. Abundant solitary wave structure can be obtained by the above analytical methods, and some numerical methods have also proved their correctness [15,16,23–26].

In different specializations of BEC, the Gross-Pitaevskii equation (GPE) has been proposed [27–30] and used to describe the wave dynamics in BEC, or the phenomena occurring in the intersection field of BEC with nonlinear optics, wave physics, and nonlinear science. Because the condensate is a good control medium for some nonlinear wave phenomena including bright-soliton, dark-soliton, four-wave mixing, and their dynamic [30], these exact or numerical soliton solutions of GPE is an important nonlinear wave model in BEC and have received extensive attention and research since the BEC first discovered in dilute atomic gases in 1995 [30–33]. Indeed, some experimental results show that stable bright soliton or dark soliton [34–38] can be excited in BEC For example, Cornish et al. [34] observed stable bright solitons in the ultra-cold 85RB BEC system by using the Feshbach resonance technique. Strecker et al. [35] and Khaykovich et al. [36] used the Feshbach resonance technique to adjust the interaction between atoms and for the first time experimentally observed stable bright solitons in BEC of ^{7}Li. Denschlag et al. [37] and Burger et al. [38] use the phase imprinting method to obtain stable bright soliton and dark soliton in BEC, respectively. Interestingly, even in experiments, theoretical research is inseparable from the GPE [36–38]. Therefore, the study of GPE provides an important reference value for predicting and describing nonlinear phenomena related to experiments, which constitutes the subject of this article.

In this article, we will study some analytical bright soliton solutions and their interaction phenomena in a high-dimensional BEC trapped in an external potential. Considering the following high-dimensional GPE [30,39,40],

$$\mathrm{i}\hbar\frac{\partial\Psi}{\partial t}=\left[-\frac{\hbar^2}{2m}\left(\frac{\partial^2}{\partial X^2}+\frac{\partial^2}{\partial Y^2}+\frac{\partial^2}{\partial Z^2}\right)+V_{\mathrm{ext}}+g|\Psi|^2\right]\Psi \tag{1}$$

where $\hbar$ is the Planck constant, $\Psi=\Psi(\mathbf{r},T)$ is the macroscopic wave function, m is mass of an atom, and external potential $V_{\mathrm{ext}}=V_{\mathrm{ext}}(\mathbf{r})$, $\mathbf{r}=(X,Y,Z)$, $\mathrm{i}^2=-1$. The coefficient g of nonlinearity strength in the GPE is given by $g=4\pi\hbar a/m$, which may be negative or positive, and this is because the scattering length is different, in the other word, one can be $a<0$ (e.g., for Li BEC) or $a>0$ (e.g., for Rb or Na BEC). In addition, it has two other terms to explain it, which correspond to focusing and defocusing nonlinearities in nonlinear optics, or to attractive and repulsive interactions between atoms, respectively [4]. The total number of atoms of GPE conserves $N=\int|\Psi|^2\mathrm{d}\mathbf{r}$. Assuming the external potential $V_{\mathrm{ext}}=m(\omega_r^2r^2+\omega_Z^2Z^2)/2$, where $\mathbf{r}^2=X^2+Y^2$, the confinement frequencies in the axial and radial directions are, respectively, ω_Z and ω_r. By separating the macroscopic wave function $\Psi=\tilde{\Psi}(X,Y,T)f(Z)$, where $[f(Z)]$ is ground state of the axial harmonic trapping potential. The system can be described by a two-dimensional GPE [39,40],

$$\mathrm{i}\hbar\frac{\partial\tilde{\Psi}}{\partial t}=\left[-\frac{\hbar^2}{2m}\left(\frac{\partial^2}{\partial X^2}+\frac{\partial^2}{\partial Y^2}\right)+\frac{m}{2}\omega_r^2r^2+g\eta\left|\tilde{\Psi}\right|^2\right]\tilde{\Psi} \tag{2}$$

where $\eta=\frac{\int[f(Z)]^4dZ}{\int[f(Z)]^2dZ}$. Introducing wave function transformation and coordinate transformation,

$$X=\sqrt{\frac{\hbar}{m\omega_z}}x,Y=\sqrt{\frac{\hbar}{m\omega_z}}y,T=\frac{t}{\omega_Z},\psi=\frac{\tilde{\Psi}\sqrt{m\omega_z}}{\sqrt{4\hbar\pi\mu_0\eta}} \tag{3}$$

here, we can choose a constant lengthμ_0, which is used to measure the scattering length of s-wave with time-dependent, then, Eq. (2) can be reduced to the following variable coefficient system [39,40],

$$\mathrm{i}\frac{\partial\psi}{\partial t}+\frac{1}{2}\left(\frac{\partial^2\psi}{\partial x^2}+\frac{\partial^2\psi}{\partial y^2}\right)-\frac{1}{2}\Omega^2(t)(x^2+y^2)\psi-\alpha(t)|\psi|^2\psi=0 \tag{4}$$

where $\Omega(t)=\omega_r/\omega_Z$ is an arbitrary function that only depends on t, ψ is the function of the time variable x, y and t,$\alpha(t)=a(t)/\mu_0$.

The study of GPE mainly lies in the difference of external potential fields. Guo et al. investigate ring dark solitons for the GPE with a harmonically trapped inhomogeneous system with time-dependent nonlinearity [41]. The soliton-like solutions in the nonlocal GPE with parity-time-symmetric external potentials are constructed by Yu [42]. Su et al. found nonautonomous solitons in the GPE with harmonic and linear external potential [43], after this, Xu and Chen studied coupled GPE with the same external potentials and their soliton solutions [44]. The couple GPE with a harmonic potential and its dark-bright soliton solutions are investigated by Alotaibi and Carr [45]. Stable light-bullet solutions and the localized spatial solitons are obtained in the harmonic and parity-time-symmetric potentials by Dai et al [46]. Dark solitons in three-component GPE by an optical dipole trap with the repulsive interactions are given by Yuan et al [47].

For a large number of nonlinear systems, including not only GPE but also Korteweg-de Vries (KdV) equation, ZK-BBM equation, Hirota-Maccari (HM) equation, etc., some interesting soliton structures are discovered via methods mentioned above, such as bell shape bright-dark soliton, rational soliton, periodic soliton, kink soliton, W-shaped soliton, V-shaped soliton, ring soliton, nonautonomous soliton and so on [18–21,39]. Moreover, in Refs. [13,14], the Hirota bilinear method is used to extract ump-periodic solitons, breather solitons in (2 + 1)-dimensional generalized fifth-order KdV equation and multi-waves solutions, exponential function solutions in (2 + 1)-dimensional Kadomtsev-Petviashvili equation, respectively. These solitons exhibit a bell-shaped soliton structures and it can understand some wave behavior in shallow water and fluid dynamics. And some approximate soliton solutions and methods for the KdV hierarchy equation [23], KdV and related problem [24] are studied by some approximate method. Some complex, hyperbolic and dark soliton solutions have been extracted for generalized Calogero-Bogoyavlenskii-Schiff equation in Ref. [22]. Refs. [25,26,48] use Abel-Riemann, Riesz-Feller, Caputo-Fabrizio fractional derivative operator to investigate soliton solutions for some different systems, respectively.

Unlike the works mentioned above, GPE (4) is a two-dimensional nonlinear equation under the BEC system, and has different external potential from GPE in Refs. [41–47]. However, most of these solitons are found in one-dimensional GPE models. In BEC, solitons in one-dimensional systems are generally considered to be stable. However, it is difficult to stabilize solitons in two-dimensional or above systems [41]. Hence, it is necessary to study the theory of high-dimensional GPE. The bell-shaped bright soliton of Eq. (4) can be stabilized via Feshbach resonance [49]. In Ref. [39], via the numerical simulation, the ring dark solitons of Eq. (4) have been studied. Ref. [40] investigates high-dimensional line rogue wave solutions for Eq. (4). However, the dynamics of detected soliton have been studied extensively, hence, discovering and investigating novel soliton structures has become one of the necessary conditions to stimulate the development of physics. Recently, new parabolic solitons and dromion-like structures solitons are discovered in the optical system [11]. To our best knowledge, soliton structures of such a kind have not been reported for two-dimensional GPE system (4). The aim and motivation of this work are to rich the exact soliton interaction structures and phenomena for high-dimensional GPE in BEC via using Hirota bilinear method. As a result, parabolic solitons, dromion-like structures, line-solitons with energy dissipation and their interaction phenomena are proposed and studied for two-dimensional GPE (4). The difference with Ref. [11] is the dynamics of interaction between two kinds soliton is investigated. These results are new in high-dimensional BEC system and may provide theoretical basis and reference for finding more stable and interesting high-dimensional soliton phenomena in BEC.

In this paper, we will construct multi-soliton solutions by the Hirota bilinear method which is introduced to deal with integrable nonlinear evolution equations in 1971 [50]. The idea was to make a transformation into new variables so that in these new variables multi-soliton solutions appear in a particularly simple form [51]. The method has undergone great development in recent years [8,9,11–14]. We'll describe detailed this approach in the next section. Therefore, in the next section, the bilinear form is given which can be used to give multi-soliton solution of the Eq. (4). In Section 3, by the Hirota bilinear method, bright multi-soliton solutions of Eq. (4) are gained. Moreover, abundant soliton interaction phenomena and their energy and amplitude changes of ones at different times are analyzed. The soliton elastic interaction is investigated via asymptotic analysis. Conclusions and future works are addressed in Section 4.

Bilinear forms and multi-soliton solutions for Eq. (4)

We will provide the exact solutions of Eq. (4) here. To this, we need to give a transformation as following [40],

$$\psi = u\left(e^{r(t)}x,\ e^{r(t)}y, t\right)e^{-\frac{i\frac{dr(t)}{dt}}{2}\left(x^2+y^2\right)+r(t)}, \Omega(t)$$
$$= \sqrt{\frac{d^2r(t)}{dt^2} - \left(\frac{dr(t)}{dt}\right)^2}, \alpha(t) = -\alpha_0, \tag{5}$$

then, a variable coefficient two-dimensional equation can be obtained [40], namely,

$$i\frac{\partial u}{\partial t} + \frac{1}{2}e^{2r(t)}\left(\frac{\partial^2 u}{\partial x^2} + \frac{\partial^2 u}{\partial y^2}\right) + \alpha_0 e^{2r(t)}|u|^2 u = 0, \tag{6}$$

where u is a continuous function that depends on time variables x,y and t, $r(t)$ is a real function that only depends on t. Accordingly, solving the exact-solution of Eq. (6) via the Hirota bilinear method and inserting it into transformation (5) can obtain the exact-solution of Eq. (4).

Bilinear forms for Eq. (6)

Firstly, we need to choose an appropriate transformation for the Hirota bilinear method. In general, the nonlinear equation in the complex domain, such as Eq. (6), consider the following transformation [51],

$$u(x, y, t) = \frac{G}{F}, \tag{7}$$

$F = F(x, y, t)$ and $G = G(x, y, t)$are, respectively, real function and complex function. Introduce the bilinear derivative operator D, namely,

$$D_x^m D_y^n D_t^p G(x, y, t) \cdot F(x, y, t)$$
$$= \left(\frac{\partial}{\partial x} - \frac{\partial}{\partial x'}\right)^m \left(\frac{\partial}{\partial y} - \frac{\partial}{\partial y'}\right)^n \left(\frac{\partial}{\partial t} - \frac{\partial}{\partial t'}\right)^p G(x, y, t)F\left(x', y', t'\right)|_{x'=x, y'=y, t'=t}, \tag{8}$$

where the parameters m, n and p are non-negative integers. Then, for the terms in Eq. (6), we have

$$\frac{\partial u}{\partial t} = \frac{\partial}{\partial t}\left(\frac{G}{F}\right) = \frac{D_t G \cdot F}{F^2}, \tag{9a}$$

$$\frac{\partial^2 u}{\partial x^2} = \frac{\partial^2}{\partial x^2}\left(\frac{G}{F}\right) = \frac{D_x^2 G \cdot F}{F^2} - \frac{G}{F}\frac{D_x^2 F \cdot F}{F^2}, \tag{9b}$$

$$\frac{\partial^2 u}{\partial y^2} = \frac{\partial^2}{\partial y^2}\left(\frac{G}{F}\right) = \frac{D_y^2 G \cdot F}{F^2} - \frac{G}{F}\frac{D_y^2 F \cdot F}{F^2}. \tag{9c}$$

Substituting Eqs. (7) and (9a)–(9c) into Eq.(6) yields

$$\mathrm{i}\frac{D_tG\cdot F}{F^2}+\frac{1}{2}\mathrm{e}^{2r(t)}\left(\frac{D_x^2G\cdot F}{F^2}-\frac{G}{F}\frac{D_x^2F\cdot F}{F^2}+\frac{D_y^2G\cdot F}{F^2}-\frac{G}{F}\frac{D_y^2F\cdot F}{F^2}\right)+\alpha_0\mathrm{e}^{2r(t)}\left|\frac{G}{F}\right|^2\frac{G}{F}=0. \tag{10}$$

Then, splitting Eq. (10) into two parts, provides the following form

$$\begin{cases}\left[\mathrm{i}D_t+\frac{1}{2}\mathrm{e}^{2r(t)}\left(D_x^2+D_y^2\right)\right]G\cdot F=0,\\ \left(D_x^2+D_y^2\right)F\cdot F=2\alpha_0GG^*,\end{cases} \tag{11}$$

which is the so-called Hirota bilinear representation of Eq. (6). Expand G and F in Eq. (7) by the following formal parameter power series

$$\begin{aligned}G&=\varepsilon g_1(x,y,t)+\varepsilon^3g_3(x,y,t)+\varepsilon^5g_5(x,y,t)+\cdots,\\ F&=1+\varepsilon^2f_2(x,y,t)+\varepsilon^4f_4(x,y,t)+\varepsilon^6f_6(x,y,t)+\cdots,\end{aligned} \tag{12}$$

where ε is an arbitrary constant. Plugging (12) into the bilinear Eq. (11) provides a polynomial for ε, and then setting whose coefficients to zero yields a recursive relation between G and F. The application for above bilinear form will be discussed in later parts.

One-soliton solution for Eq. (4)

To secure the one-soliton solution of Eq. (4), we set $g_1(x,y,t)=C_1\mathrm{e}^{\eta_1}$, where C_1 is any complex number. Then, consider the following expansion form to (7) given by

$$G=\varepsilon g_1(x,y,t),F=1+\varepsilon^2f_2(x,y,t), \tag{13}$$

where $\eta_1=\mu_1x+\nu_1y+c_1(t)+\kappa_1$, μ_1, ν_1, $\kappa_1$are complex constants and $c_1(t)$ is complex function. From the knowledge of Hirota bilinear method, let all coefficients of ε and ε^2 be equal to zero, then we get the following set of algebraic equations

$$\begin{cases}\mathrm{i}\mathrm{e}^{-2r(t)}\frac{\partial}{\partial t}g_1+\frac{1}{2}\frac{\partial^2}{\partial x^2}g_1+\frac{1}{2}\frac{\partial^2}{\partial y^2}g_1=0,\\ -\alpha_0|g_1|^2+\frac{1}{2}\frac{\partial^2}{\partial x^2}f_2+\frac{1}{2}\frac{\partial^2}{\partial y^2}f_2=0.\end{cases} \tag{14}$$

Solving Eq. (14) has

$$f_2(x,y,t)=n_1\mathrm{e}^{\eta_1+\eta_1^*},n_1=\frac{|C_1|^2\alpha_0}{(\mu_1+\mu_1^*)^2+(\nu_1+\nu_1^*)^2},c_1(t)=\frac{\mathrm{i}\left(\mu_1^2+\nu_1^2\right)}{2}\int\mathrm{e}^{2r(t)}\mathrm{d}t. \tag{15}$$

Setting $\varepsilon=1$, solution (7) of Eq. (6) may be expressed as

$$u(x,y,t)=\frac{C_1\mathrm{e}^{\eta_1}}{1+n_1\mathrm{e}^{\eta_1+\eta_1^*}}. \tag{16}$$

Thus, from (5), the one-soliton solution of Eq. (4) may be written as

$$\psi=u(\mathrm{e}^{r(t)}x,\mathrm{e}^{r(t)}y,t)\mathrm{e}^{-\frac{\mathrm{i}\mathrm{d}r(t)}{2\,\mathrm{d}t}(x^2+y^2)+r(t)}. \tag{17}$$

In the next section, we will give the explicit expression of one-soliton solution (17) and discuss their structures.

Two-soliton solution for Eq. (4)

To secure two-soliton solution of Eq. (4), we assume that $g_1(x,y,t)=C_1\mathrm{e}^{\eta_1}+C_2\mathrm{e}^{\eta_2}$ and make the coefficient of ε, ε^2, ε^3 and ε^4 be equal to zero, where C_1 and C_2 are any complex numbers. Hence, we can get the following set of algebraic equations,

$$\begin{cases}\mathrm{i}\mathrm{e}^{-2r(t)}\frac{\partial}{\partial t}g_1+\frac{1}{2}\frac{\partial^2}{\partial x^2}g_1+\frac{1}{2}\frac{\partial^2}{\partial y^2}g_1=0,\\ -\alpha_0|g_1|^2+\frac{1}{2}\frac{\partial^2}{\partial x^2}f_2+\frac{1}{2}\frac{\partial^2}{\partial y^2}f_2=0,\\ \frac{1}{2}\left(\frac{\partial^2}{\partial x^2}+\frac{\partial^2}{\partial y^2}\right)(g_1f_2+g_3)-\left(\frac{\partial}{\partial x}g_1\right)\frac{\partial}{\partial x}f_2-\left(\frac{\partial}{\partial y}g_1\right)\frac{\partial}{\partial y}f_2-\mathrm{i}\mathrm{e}^{-2r(t)}\left[f_2\frac{\partial}{\partial t}g_1-g_1\frac{\partial}{\partial t}f_2+\frac{\partial}{\partial t}g_3\right]=0,\\ f_2\left(\frac{\partial^2}{\partial x^2}+\frac{\partial^2}{\partial y^2}\right)f_2-\left(\frac{\partial}{\partial x}f_2\right)^2-\left(\frac{\partial}{\partial y}f_2\right)^2+\left(\frac{\partial^2}{\partial x^2}+\frac{\partial^2}{\partial y^2}\right)f_4-\alpha_0\left(g_3g_1^*+g_1g_3^*\right)=0.\end{cases} \tag{18}$$

Then, g_3,f_2 and f_4 can be solved with the aid of Maple, and they are listed in **Appendix A**. Setting $\varepsilon=1$, two-soliton solution (7) of Eq. (6) takes the following form,

$$u(x,y,t)=\frac{g_1+g_3}{1+f_2+f_4}, \tag{19}$$

where the exponent (R) and (I) in the parameter denote its real part and imaginary part, respectively. Thus, the two-soliton solution of Eq. (4) is rewritten as

$$\psi=u(\mathrm{e}^{r(t)}x,\mathrm{e}^{r(t)}y,t)\mathrm{e}^{-\frac{\mathrm{i}\mathrm{d}r(t)}{2\,\mathrm{d}t}(x^2+y^2)+r(t)}, \tag{20}$$

where

$$u(x,y,t)=\frac{C_1\mathrm{e}^{\eta_1}+C_2\mathrm{e}^{\eta_2}+m_1\mathrm{e}^{\eta_1+\eta_2+\eta_1^*}+m_2\mathrm{e}^{\eta_1+\eta_2+\eta_2^*}}{1+n_1\mathrm{e}^{\eta_1+\eta_1^*}+n_2\mathrm{e}^{\eta_2+\eta_2^*}+n_3\mathrm{e}^{\eta_1+\eta_2^*}+n_4\mathrm{e}^{\eta_2+\eta_1^*}+n_5\mathrm{e}^{\eta_1+\eta_1^*+\eta_2+\eta_2^*}}. \tag{21}$$

We will discuss the interaction of two-soliton solution (21) in the next section.

Three-soliton solution for Eq. (4)

Assume that $g_1(x,y,t)=C_1\mathrm{e}^{\eta_1}+C_2\mathrm{e}^{\eta_2}+C_3\mathrm{e}^{\eta_3}$, C_1, C_2 and C_3 are any complex numbers. Then, collecting the coefficients of ε, ε^2, ε^3, ε^4,ε^5 and ε^6 and setting them to zero can yield a set of algebraic equations, here we omit it due to its complexity. The three-soliton solution can be obtained as

$$u(x,y,t)=\frac{g_1+g_3+g_5}{1+f_2+f_4+f_6}, \tag{22}$$

where the expressions of g_3,g_5,f_2,f_4 and f_6 are listed in **Appendix B**. Therefore, the three-soliton solution of Eq. (4) may be obtained as

$$\psi=u(\mathrm{e}^{r(t)}x,\mathrm{e}^{r(t)}y,t)\mathrm{e}^{-\frac{\mathrm{i}\mathrm{d}r(t)}{2\,\mathrm{d}t}(x^2+y^2)+r(t)}. \tag{23}$$

We will discuss the structures of three-soliton solution in the next section.

Discussion on soliton structures and interactions

One-soliton solution and parameter analysis

As previously stated, one-, two- and three-soliton solutions of Eq. (4) have already constructed. In order to understand their dynamics, their graphical representations under different parameters will be exhibited in this section.

Rewrite one-soliton solution (17) of Eq. (6) as

$$u(x,y,t)=\frac{C_1\mathrm{e}^{\mathrm{i}\left[\mu_1^{(\mathrm{I})}x+\nu_1^{(\mathrm{I})}y+c_1^{(\mathrm{I})}(t)+\kappa_1^{(\mathrm{I})}\right]}}{2\sqrt{n_1}}\mathrm{sech}\left(\mu_1^{(\mathrm{R})}x+\nu_1^{(\mathrm{R})}y+c_1^{(\mathrm{R})}(t)+\kappa_1^{(\mathrm{R})}+\frac{1}{2}\ln n_1\right). \tag{24}$$

By transformation (5), the one-soliton solution of two-dimensional GPE (4) can be written as

$$\begin{aligned}\psi&=u\left(\mathrm{e}^{r(t)}x,\mathrm{e}^{r(t)}y,t\right)\mathrm{e}^{-\frac{\mathrm{i}\mathrm{d}r(t)}{2\,\mathrm{d}t}\left(x^2+y^2\right)+r(t)}\\ &=\frac{C_1\mathrm{e}^{r(t)}\mathrm{e}^{\mathrm{i}h(x,y,t)}}{2\sqrt{n_1}}\mathrm{sech}\left(\mu_1^{(\mathrm{R})}\mathrm{e}^{r(t)}x+\nu_1^{(\mathrm{R})}\mathrm{e}^{r(t)}y+c_1^{(\mathrm{R})}(t)+\kappa_1^{(\mathrm{R})}+\frac{1}{2}\ln n_1\right),\end{aligned} \tag{25}$$

where $h(x,y,t)=\mu_1^{(\mathrm{I})}\mathrm{e}^{r(t)}x+\nu_1^{(\mathrm{I})}\mathrm{e}^{r(t)}y+c_1^{(\mathrm{I})}(t)+\kappa_1^{(\mathrm{I})}-\frac{1}{2}\frac{\mathrm{d}r(t)}{\mathrm{d}t}(x^2+y^2)$ is a real function. Note that the motion of the soliton (25) depends

on both x and t, y and t, x and y according to variables μ_1, v_1,$c_1(t)$,κ_1 and $r(t)$, and it elucidates the soliton amplitude is $\left|\frac{C_1 e^{r(t)}}{2\sqrt{n_1}}\right|$. The one-soliton structure can be divided into the two categories:

(1) When $r(t)$ does not depend on t, in other words, $r(t) = \chi$ is a constant function, one-soliton solution shows common bell-shaped soliton structures without amplitude variation;
(2) When $r(t)$ depents on t, the one-soliton solution has abundant structures and its amplitude is variational, we will discuss it here.

In the analytic one-soliton solution of Eq. (25), there are five parameters μ_1, v_1, κ_1, C_1, α_0 and one variable coefficient function $e^{r(t)}$. Before analyzing soliton interactions, we assign $e^{r(t)} = \cos(\arctan t)$, the structures of the distinct wave functions ψ when$y = 1$ with respect to radial coordinate x and time t are demonstrated in Fig. 1. The effects of other parameters on the structure of one-soliton is as follow:

- Fig. 1a exhibits one bright parabolic soliton structure which represents the dynamic process of matter waves condensing from a position in the field and then annihilating to the same position when $\mu_1 = -2$, $v_1 = -1$, $\kappa_1 = -1 + 5\mathrm{i}$, $\alpha_0 = 2$, $C_1 = 1$ and $y = 1$ are chosen. With the evolution of time, the energy of the matter wave function in the field will gradually concentrate at the vertex of the parabolic soliton and then disappear into the field. It shows distinct dynamical feature from the parabolic wave soliton in Refs. [18,21].
- Fig. 1b exhibits a line-soliton when we change μ_1 from -2 to $-1 + 5\mathrm{i}$ on the basis of Fig. 1a, while others are retained as before. The radian of the parabolic soliton in Fig. 1a will gradually decrease and become almost line-soliton. In comparison to the general bell-shapes line-solitons in Refs. [18,20,21], which can achieve the purpose of long-distance transmission in the physical environment according to their dynamics, the amplitude and energy of the line-solitons found here decay from the center to the sides. It shows that the energy of the matter wave soliton starts to gather from one side of the field to the origin, and then annihilates to the other side. It described vividly the energy accumulation of waves is from the field and then dissipated into infinity.
- Fig. 1c shows a dromion-like structure when we replace the $\kappa_1 = -1 + 5i$ with $\kappa_1 = 1 + 5\mathrm{i}$ on the basis of Fig. 1a, whose structure describes the concentrated energy in the center of the field. This represents the dynamics of matter wave soliton with concentration of energy, which can simulate the condensed structure of N atoms $(N = \int |\psi|^2 \mathrm{d}x)$. The energy of the

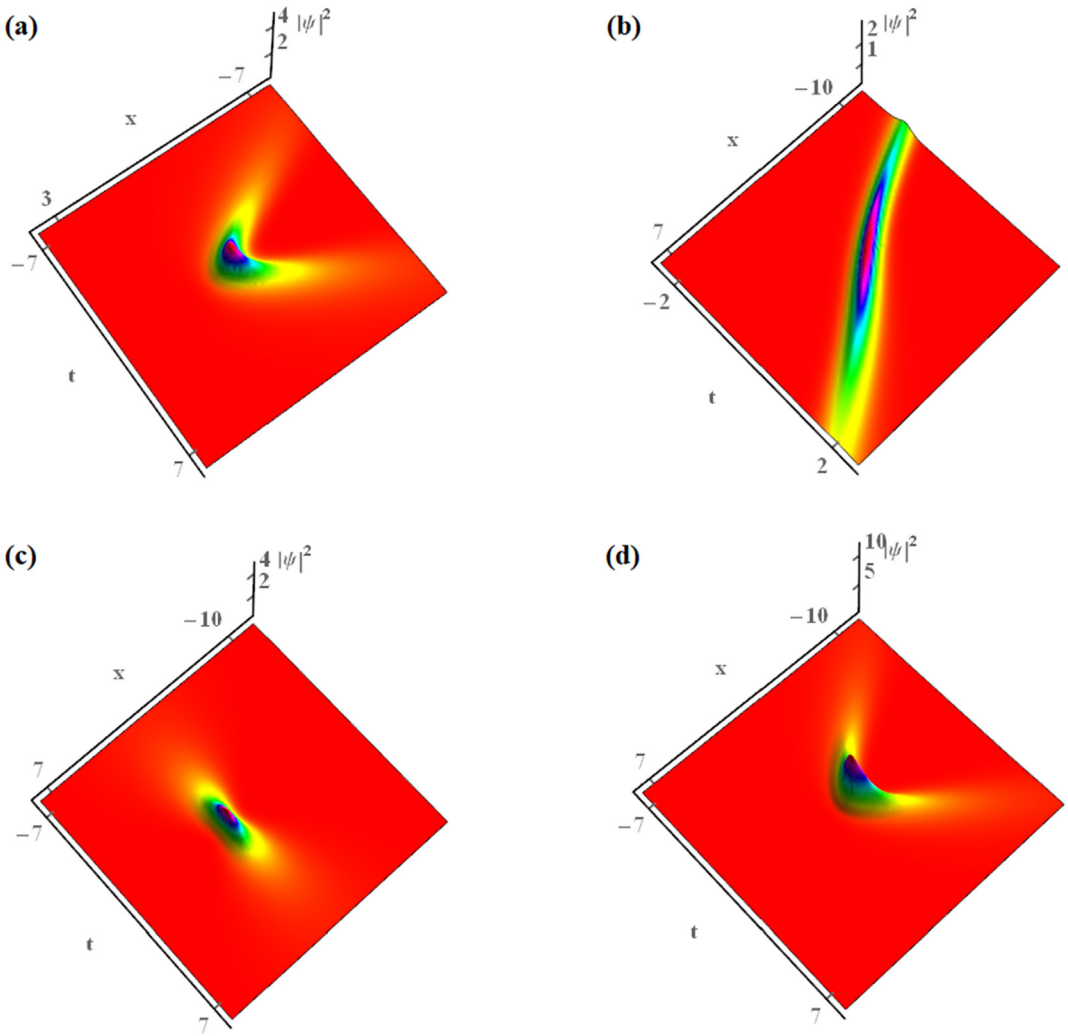

Fig. 1. One-soliton solution (25) for $y = 1$ with same parameters $v_1 = -1$, $C_1 = 1$ and different parameters **(a)** $\mu_1 = -2$, $\kappa_1 = -1 + 5\mathrm{i}$, $\alpha_0 = 2$; **(b)** $\mu_1 = -1 + 5\mathrm{i}$, $\kappa_1 = -1 + 5\mathrm{i}$, $\alpha_0 = 2$; **(c)** $\mu_1 = -2$, $\kappa_1 = 1 + 5\mathrm{i}$, $\alpha_0 = 2$; **(d)** $\mu_1 = -2$, $\kappa_1 = -1 + 5\mathrm{i}$, $\alpha_0 = \frac{1}{2}$.

atoms at different time t_0 is $E = \int |\psi(x, t_0)|^2 dx$. Interestingly, this soliton structure is very similar to the structure of atomic condensed matter observed in experiments [31].

- Fig. 1d shows different amplitude one parabolic soliton from Fig. 1a when we adjust the parameter $\alpha_0 = 2$ to $\alpha_0 = \frac{1}{2}$ on the basis of Fig. 1a. Due to the different parameter α_0, the amplitude of matter wave soliton decreases. The shape of the soliton shows the same dynamic process as Fig. 1a. The structures of these solutions in Fig. 1 exhibit a smooth profile at any time, it has different dynamics with nonsmooth solitons at their peak [19,21]. In other words, the left and right derivatives of soliton in Fig. 1 are equal at its peak, whereas the nonsmooth soliton is not equal [52]. Smooth solitons are more easily excited and stable in experiments, and have good physical properties.

The energy of above one-soliton is $E = \int |\psi|^2 dx$ for $y = 1$, which is just the total number of atoms of GPE and their energy will concentrate at the peak gradually. Without loss of generality, the effects of parameters on the soliton structure are exhibited in Fig. 2. Fig. 2a, b and c exposes the direction of rotation or translation of the parabolic soliton with the parameters change. As we can see in Fig. 2a, b and c, the solid arrows point to the rotation direction of the two sides of the parabolic soliton, which have different linear velocities, and the dashed arrows point to its translation direction. Small arrows '↑' and '↓' after parameters indicate increasing and decreasing them, respectively. As an example, when we increase the imaginary part of μ_1 (i.e. $\mu_1^{(I)}$) in Fig. 1a, parabolic soliton becomes line-soliton (see Fig. 1a and b). Meanwhile, the larger the value of the $\mu_1^{(R)}$ and $v_1^{(I)}$ the bigger the amplitude. On the contrary, the larger the value of α_0, the smaller the amplitude. The corresponding cross sections in 1a and 1d using different α_0 are shown in Fig. 2d. The imaginary part of κ_1(i.e. $\kappa_1^{(I)}$) cannot affect any structure of the one-soliton. Different processes of energy concentration of one-soliton can be obtained by adjusting the relevant parameters.

Remark 1. The feature of these solutions is that the energy is gathered from the field and then dissipated into the field. Therefore, the structure and shape of these bright solitons can vividly describe the dynamic process of cold atom condensation in single BEC system. By analyzing the wave function expression and Fig. 2, different atomic condensation states can be obtained. It can be seen from expression (25) that the energy condensation time in the experiment is controllable theoretically by correction of relevant parameters.

Two-soliton solution interaction analysis

Based on the above analysis, we can also give some interaction phenomena of two- and three-soliton. In order to find whether the elastic interaction between the two solitons is preserved in the presence of variable coefficient, we perform an asymptotic analysis of solution, which is a necessary step to investigate the dynamics of two-soliton. Modelled on the method in Refs. [53,54], computing four limit can lead to the following four types of asymptotic patterns:

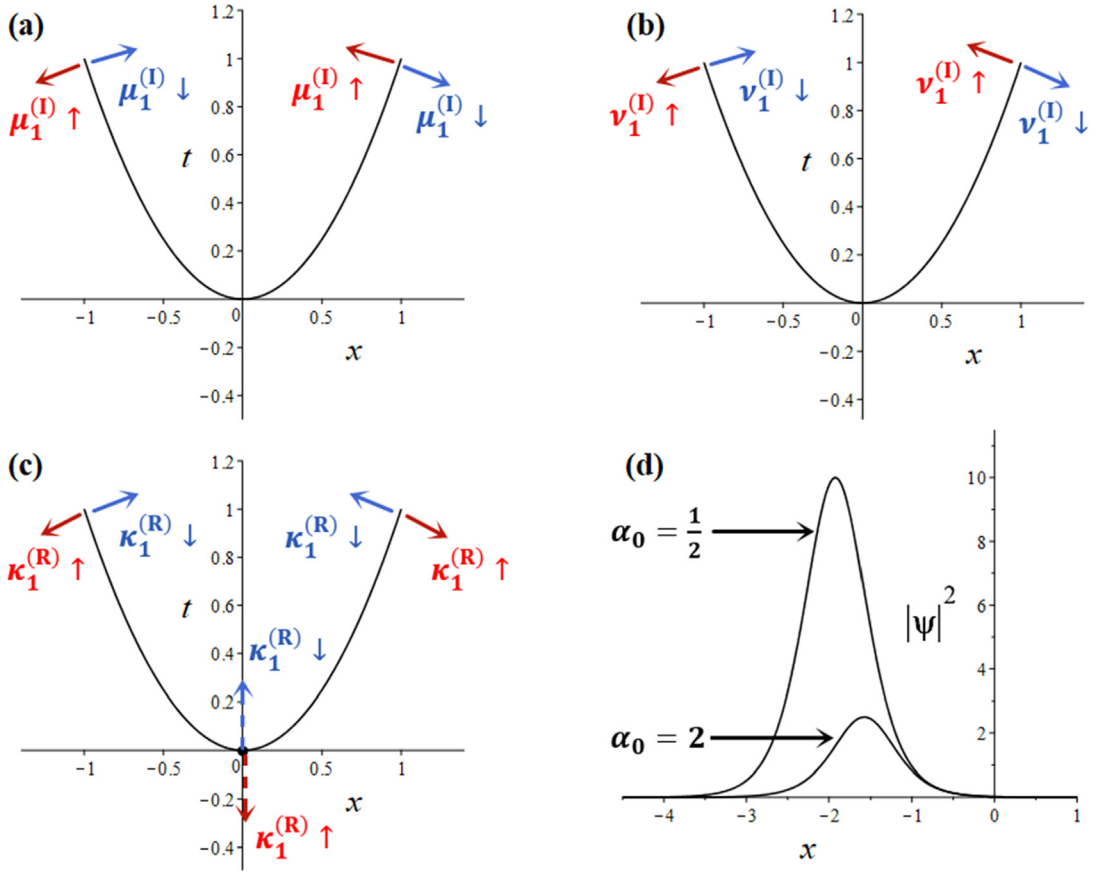

Fig. 2. Phase diagram for the direction of rotation or translation of parabolic soliton with parameters change. The small arrows '↑' and '↓' after the parameters represent increasing and decreasing the corresponding parameters, respectively. The solid arrows and dashed arrows express the direction of rotation and translation, respectively.

(i) Before the interactions

As $\eta_1+\eta_1^*\sim 0$, $\eta_2+\eta_2^*\to-\infty$, then

$$\psi^{1-}=\frac{C_1e^{r(t)}e^{ih_1(x,y,t)}}{2\sqrt{n_1}}\operatorname{sech}\left[\mu_1^{(R)}e^{r(t)}x+v_1^{(R)}e^{r(t)}y+c_1^{(R)}(t)+\kappa_1^{(R)}+\frac{1}{2}\ln n_1\right];$$

As $\eta_1+\eta_1^*\sim+\infty$, $\eta_2+\eta_2^*\to 0$, then

$$\psi^{2-}=\frac{m_1e^{r(t)}e^{ih_2(x,y,t)}}{2n_5\sqrt{\frac{n_1}{n_5}}}\operatorname{sech}\left[\mu_2^{(R)}e^{r(t)}x+v_2^{(R)}e^{r(t)}y+c_2^{(R)}(t)+\kappa_2^{(R)}-\frac{1}{2}\ln\frac{n_1}{n_5}\right];$$

(ii) After the interactions

As $\eta_1+\eta_1^*\sim 0$, $\eta_2+\eta_2^*\to+\infty$, then

$$\psi^{1+}=\frac{m_2e^{r(t)}e^{ih_1(x,y,t)}}{2n_5\sqrt{\frac{n_2}{n_5}}}\operatorname{sech}\left[\mu_1^{(R)}e^{r(t)}x+v_1^{(R)}e^{r(t)}y+c_1^{(R)}(t)+\kappa_1^{(R)}-\frac{1}{2}\ln\frac{n_2}{n_5}\right];$$

As $\eta_1+\eta_1^*\sim-\infty$, $\eta_2+\eta_2^*\to 0$, then

$$\psi^{2+}=\frac{C_2e^{r(t)}e^{ih_2(x,y,t)}}{2\sqrt{n_2}}\operatorname{sech}\left[\mu_2^{(R)}e^{r(t)}x+v_2^{(R)}e^{r(t)}y+c_2^{(R)}(t)+\kappa_2^{(R)}+\frac{1}{2}\ln n_2\right],$$

where $h_j(x,y,t)=\mu_j^{(I)}e^{r(t)}x+v_j^{(I)}e^{r(t)}y+c_j^{(I)}(t)+\kappa_j^{(I)}-\frac{1}{2}\frac{dr(t)}{dt}(x^2+y^2)$, here$j=1,2$. From their asymptotic forms, it is found that the amplitudes, velocities and structures of each soliton remain unchangeable even upon mutual interaction, except for the initial phase. Hence, we can easily see that the interactions of two-soliton solutions are elastic. In obedience to similarity between the asymptotic expressions and one-soliton (25), we may still choose the appropriate parameters to give different two-soliton structures according to the previous analysis.

Table 1 summarizes the amplitude and initial phase of four asymptotic patterns $\psi^{1\pm}$ and $\psi^{2\pm}$ of two-soliton (21) when the y is fixed. Amplitude has a great influence on the energy spectrum of solitons. Thus, according to the results of Fig. 2 and Table 1, we can choose some appropriate parameters to make multiple solitons with different amplitude, energy, shape, and phase interact with others elastically. So as to provide theoretical results and references for the multi-soliton phenomenon in the experiment.

Fig. 3 illustrates that two-soliton interaction phenomena among parabolic solitons, line-solitons and dromion-like structures. Set $e^{r(t)}=\cos(\arctan t)$ and $C_1=C_2=1$, $\alpha_0=2$, $y=1$, and discuss the effect of other parameters on the structure as follow:

- Fig. 3a depicts the interactional shape of two parabolic solitons with the same opening for the free parameters $\mu_1=-1$, $v_1=1$, $\kappa_1=-1$, $\mu_2=-2$, $\kappa_2=-1$, $\alpha_0=2$. It represents the collision dynamics of two bright solitons with parabolic shapes. Now, as a function of the initial phase ψ^{1-} and ψ^{2-}, they start to condense energy from the same spaces and different times.

Table 1
Amplitude and initial phase of the four asymptotic patterns of two-soliton (21) for fixed y and $r(t)$.

	Soliton	Amplitude	Initial phase
Before interaction	ψ^{1-}	$\left\|\frac{C_1e^{r(t)}}{2\sqrt{n_1}}\right\|$	$c_1^{(R)}(0)+v_1^{(R)}e^{r(0)}y+\kappa_1^{(R)}+\frac{1}{2}\ln n_1$
	ψ^{2-}	$\left\|\frac{m_1e^{r(t)}}{2n_5\sqrt{n_1/n_5}}\right\|$	$c_2^{(R)}(0)+v_2^{(R)}e^{r(0)}y+\kappa_2^{(R)}-\frac{1}{2}\ln\frac{n_1}{n_5}$
Afterinteraction	ψ^{1+}	$\left\|\frac{m_2e^{r(t)}}{2n_5\sqrt{n_2/n_5}}\right\|$	$c_1^{(R)}(0)+v_1^{(R)}e^{r(0)}y+\kappa_1^{(R)}-\frac{1}{2}\ln\frac{n_2}{n_5}$
	ψ^{2+}	$\left\|\frac{C_2e^{r(t)}}{2\sqrt{n_2}}\right\|$	$c_2^{(R)}(0)+v_2^{(R)}e^{r(0)}y+\kappa_2^{(R)}+\frac{1}{2}\ln n_2$

- Fig. 3b depicts the interactional shape of two parabolic solitons with the different opening when μ_2 is changed from -2 to 2 on the basis of parameters of Fig. 3a, while others remain unchanged. The opening of one soliton turns to the opposite. It represents the collision dynamics of two bright solitons with parabolic shapes. they start to condense energy from the same times and different spaces.
- Fig. 3c exhibits the two-soliton interactional shape between one parabolic soliton and one dromion-like structure when we adjust κ_1 from -1 to 1 on the basis of Fig. 3b. This structure can simulate the energy accumulation process of a parabolic soliton into another condensed matter wave. When the parabolic soliton energy is dissipated, the structure of the original matter wave at the center of the field is not affected.
- Fig. 3d exhibits the interaction of one line-soliton and one parabolic soliton when we change the μ_2 from 2 to $-\frac{1}{2}+6i$, κ_2 from -1 to -2 on the basis of Fig. 3b. The amplitude of near the vertex of parabolic soliton is periodic oscillation when the line-soliton passes through it near the center of the field. This can simulate the process in which parabolic soliton and linear soliton gather energy at the same field.
- Fig. 3e shows the interactional shape of one line-soliton and one dromion-like structure for the parameters $\mu_1=v_1=1+2i$, $\kappa_1=0.56$, $\mu_2=-1.3$,$\kappa_2=0.56$. Interacting between them at the center of field makes the energy of the dromion-like structure transfer to the line-soliton, and present a new peak and two depressions. After the interaction, the line-soliton returns to original structure (see Fig. 3e). This can simulate the process of an energy beam (one line-solitons) passing through the condensate and allow the condensate amplification and compression.
- Fig. 3f shows interaction of two line-solitons when we change the $\kappa_1=\kappa_2=0.56$ to $\kappa_1=\kappa_2=0$, $\mu_2=-1.3$ to $\mu_2=-1.9+i$ on the basis of parameters of Fig. 3e. Interacting between them makes the energy and amplitude reach a new height. After their interaction, they return to their original structure and continue to propagate.

According to the results of asymptotic analysis and graph analysis, the two solitons here are all shown to be the most classical soliton characteristic----elastic interaction. Although the amplitude and energy of the soliton is affected by the random function $r(t)$, the interaction does not affect the original physical characteristics of each soliton. As shown in the above two soliton interactions, different soliton interactions show more abundant and interesting dynamics and structures. The elastic soliton interactions play an important role in practical applications and experiments. The solitons show same waveforms and propagation directions after their interaction. To better understand the dynamics of their propagation and elastic interaction, we plot energy evolution of soliton and interaction process in Figs. 4 and 5, respectively.

Fig. 4 shows the energy change of one- and two-soliton $|\psi|^2$. Here, $E=\int_{-\infty}^{\infty}|\psi(x,t_0)|^2dx$ denotes the energy of $|\psi|^2$. Apparently, from Fig. 4, the soliton reach its maximum value of the energy is at $t=0$, which is in good agreement with the maximum amplitude of the soliton at $t=0$ in the three-dimensional structures of solitons (see Figs. 1 and 3). After they gather ($t>0$), their energy diminishes and spreads out into the field. Therefore, in Fig. 5, we plot the evolution process of soliton interaction at $t=0$ and $t>0$. As can be seen from Fig. 5, the blue solid-lines represent the shape of the two-solitons when the energy concentration is completed. The two solitons interaction can reach a new amplitudes that are not directly related to $\psi^{1\pm}$ or $\psi^{2\pm}$. This is a specific moment which the two-soliton reaches its maximum amplitude

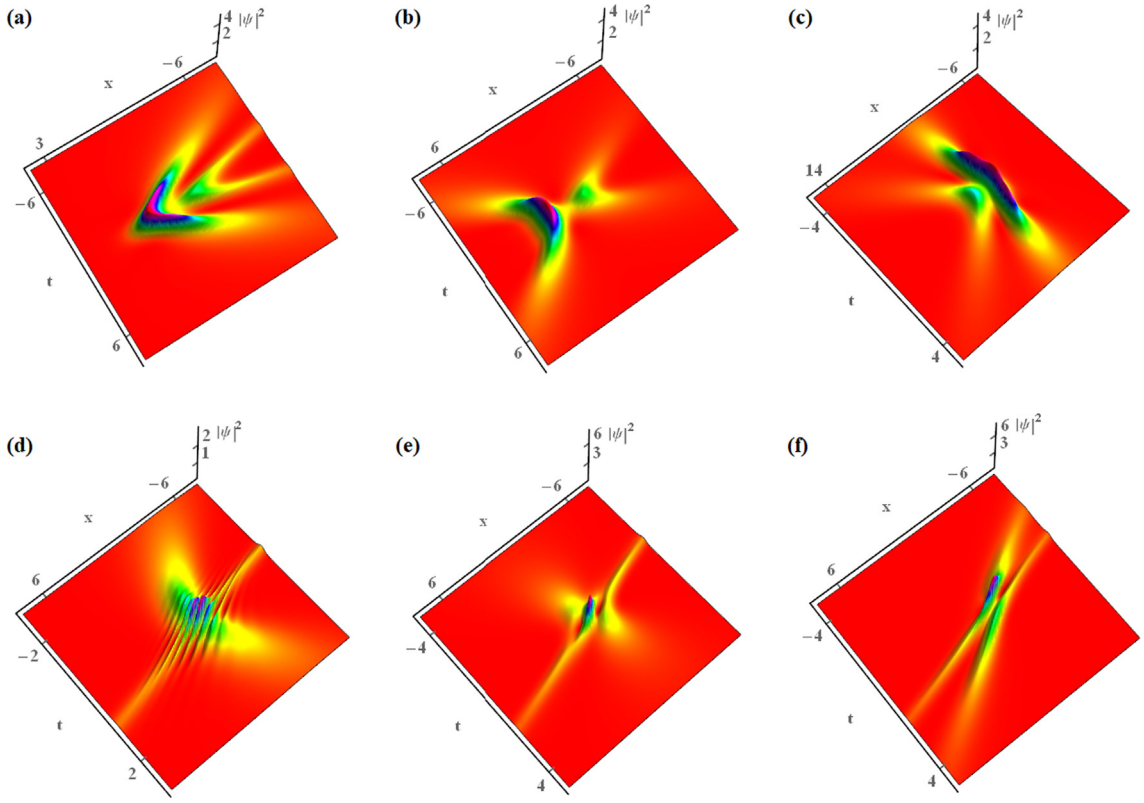

Fig. 3. Two-soliton solution (21) for $y = 1$ with same parameters $C_1 = C_2 = 1$, $\alpha_0 = 2$ and different parameters **(a)** $\mu_1 = -1$, $\nu_1 = 1, \kappa_1 = -1, \mu_2 = -2, \kappa_2 = -1$; **(b)** $\mu_1 = -1$, $\nu_1 = 1, \kappa_1 = -1, \mu_2 = 2, \kappa_2 = -1$; **(c)** $\mu_1 = -1$, $\nu_1 = 1, \kappa_1 = 1, \mu_2 = 2, \kappa_2 = -1$; **(d)** $\mu_1 = -1$, $\nu_1 = 1, \kappa_1 = -1, \mu_2 = -\frac{1}{2} + 6\mathrm{i}, \kappa_2 = -2$; **(e)** $\mu_1 = 1 + 2\mathrm{i}$, $\nu_1 = 1 + 2\mathrm{i}, \kappa_1 = 0.56, \mu_2 = -1.3, \kappa_2 = 0.56$; **(f)** $\mu_1 = 1 + 2\mathrm{i}$, $\nu_1 = 1 + 2\mathrm{i}, \kappa_1 = 0, \mu_2 = -1.9 + \mathrm{i}, \kappa_2 = 0$.

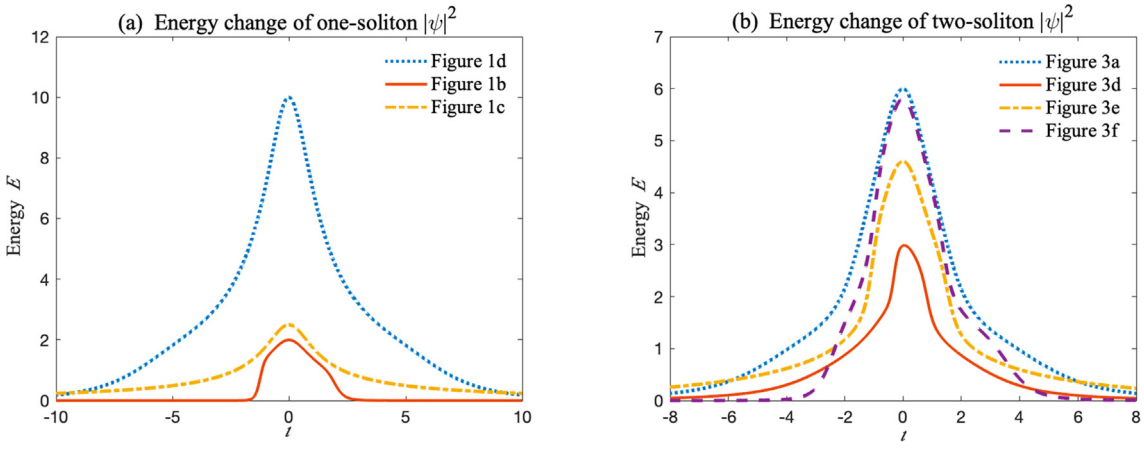

Fig. 4. The energy evolution of (a) three types (Fig. 1d, Fig. 1b and Fig. 1c) of one-soliton $|\psi|^2$ and (b) four types (Fig. 3a, Fig. 3d, Fig. 3e and Fig. 3f) of two-soliton $|\psi|^2$ with the different time t_0 (defining energy $E = \int_{-\infty}^{\infty} |\psi(x, t_0)|^2 \mathrm{d}x$).

and energy, and the wave function at this time can simulate the condensed state of cold atoms. The red dotted-lines represent the states of the two-solitons after their interaction. We can also plot the motion of solitons at other times, and observe the process of their energy annihilation in this regime. This makes it possible to control the energy and accumulation rate of matter waves in experiments.

Remark 2. These nonlinear interactions show the different energy concentration processes of multiple solitons. Two solitons ψ^{1-} and ψ^{2-} condense their energy from the initial phases in space to the center of field, and then they annihilate from their interaction points to the initial phases of two solitons ψ^{1+} and ψ^{2+}. The energy of two solitons at time t_0 are $E_{1-} = \int |\psi^{1-}(x, t_0)|^2 \mathrm{d}x$ and $E_{2-} = \int |\psi^{2-}(x, t_0)|^2 \mathrm{d}x$ before their interaction, and $E_{1+} = \int |\psi^{1+}(x, t_0)|^2 \mathrm{d}x$ and $E_{2+} = \int |\psi^{2+}(x, t_0)|^2 \mathrm{d}x$ after their interaction. The elastic interaction phenomenon of solitons with distinct shapes in Fig. 3 may simulate the complex nonlinear phenomenon of condensed matter waves in some real experiments. This makes it theoretically possible to control the position of the multiple matter waves, the condensate and annihilation process in the experiment.

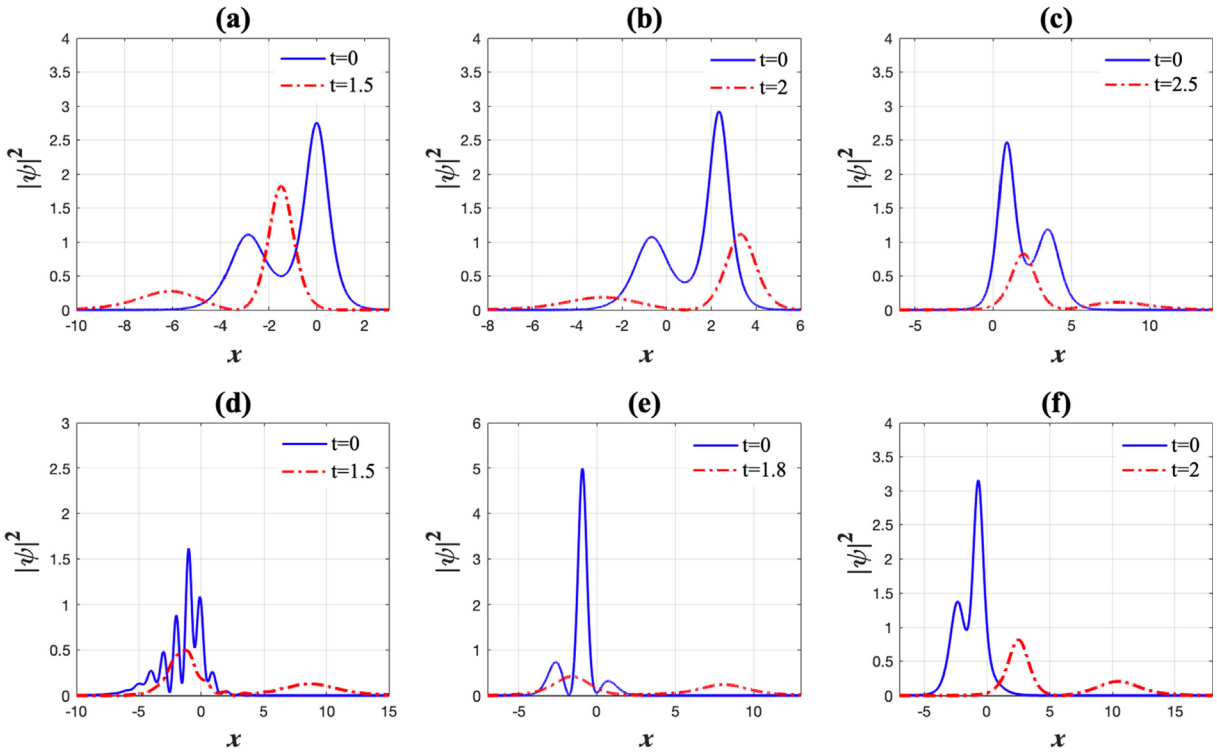

Fig. 5. The interaction process of two-soliton $|\psi|^2$ during interaction ($t = 0$) and after interaction ($t > 0$). (a), (b), (c), (d), (e) and (f) correspond to Fig. 3a-3f respectively.

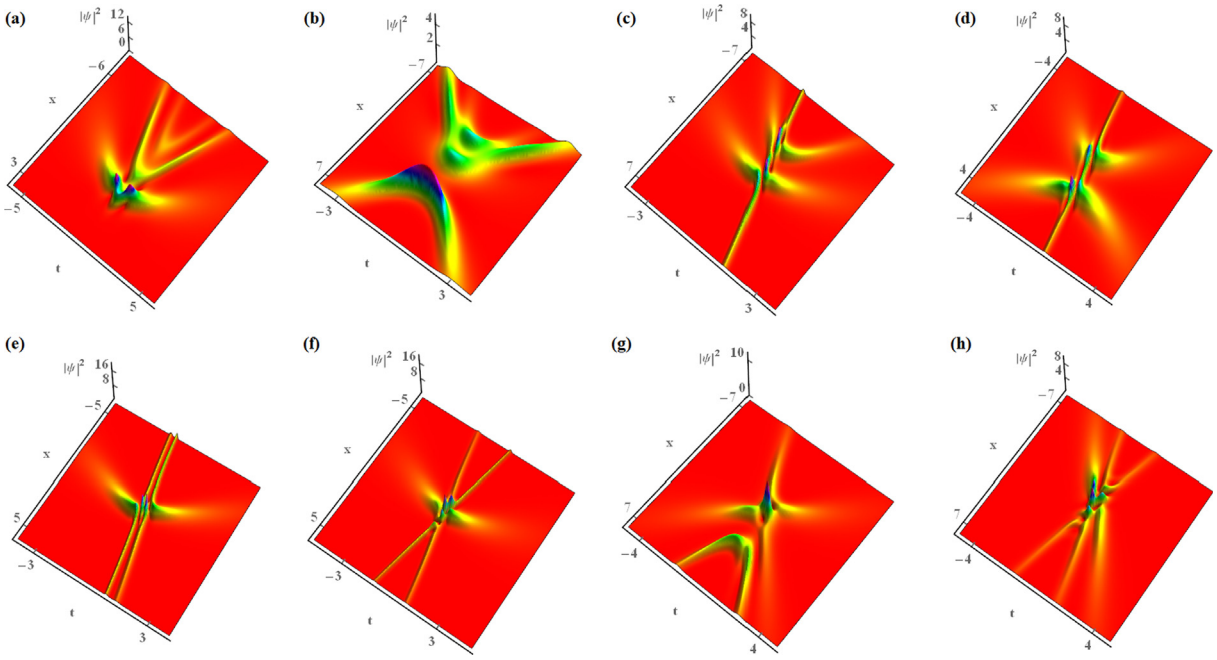

Fig. 6. Three-soliton solution (23) for $y = 1$ with same parameters $C_1 = C_2 = C_3 = 1$ and different parameters **(a)** $\mu_1 = -1$, $\nu_1 = 1$,$\kappa_1 = -1$,$\mu_2 = -2$,$\kappa_2 = -1$, $\mu_3 = -3$, $\kappa_3 = -1$, $\alpha_0 = 2$; **(b)** $\mu_1 = -1.1$, $\nu_1 = 1$,$\kappa_1 = -1$,$\mu_2 = 2$,$\kappa_2 = -1$, $\mu_3 = -\frac{11}{5}$, $\kappa_3 = 0$, $\alpha_0 = 2$; **(c)** $\mu_1 = -1.6$, $\nu_1 = 1$,$\kappa_1 = 0$,$\mu_2 = -\frac{11}{5}$,$\kappa_2 = 0$, $\mu_3 = -2 + 4\mathrm{i}$, $\kappa_3 = 0$, $\alpha_0 = 2$; **(d)** $\mu_1 = -3$, $\nu_1 = 1$,$\kappa_1 = 0$,$\mu_2 = \frac{11}{5}$,$\kappa_2 = 0$, $\mu_3 = \frac{8}{5} + 4\mathrm{i}$, $\kappa_3 = 0$, $\alpha_0 = 2$; **(e)** $\mu_1 = -3$, $\nu_1 = 2$,$\kappa_1 = 0$,$\mu_2 = -\frac{11}{5} + 5\mathrm{i}$,$\kappa_2 = 0$, $\mu_3 = -2 + 4\mathrm{i}$, $\kappa_3 = 0$, $\alpha_0 = 2$; **(f)** $\mu_1 = -3$, $\nu_1 = 1$,$\kappa_1 = 0$,$\mu_2 = -\frac{11}{5} - 5\mathrm{i}$,$\kappa_2 = 0$, $\mu_3 = \frac{9}{5} + 4\mathrm{i}$, $\kappa_3 = 0$, $\alpha_0 = 2$; **(g)** $\mu_1 = 1.8 - \mathrm{i}$, $\nu_1 = \frac{1}{2} + \frac{\mathrm{i}}{3}$,$\kappa_1 = 0$,$\mu_2 = -1.5 + 1.8\mathrm{i}$,$\kappa_2 = 0$, $\mu_3 = 2 - \frac{3\mathrm{i}}{4}$, $\kappa_3 = 0$, $\alpha_0 = 1$; **(h)** $\mu_1 = 1 + 2\mathrm{i}$, $\nu_1 = 1 + 2\mathrm{i}$,$\kappa_1 = 0$,$\mu_2 = -1.7 + \mathrm{i}$,$\kappa_2 = 0$, $\mu_3 = 0.89 - 2.7\mathrm{i}$, $\kappa_3 = 0$, $\alpha_0 = 2$.

Three-soliton solution interaction analysis

Fig. 6 shows distinct three-soliton structures. By choosing appropriate parameters, we can also obtain the interaction of multi-soliton, including the following cases:

- Fig. 6a displays the collision dynamics of three parabolic solitons with same openings. It describes the condensation of three different groups of cold atoms in the field from the same position towards the center of the field at different times.

- Fig. 6b displays the collision dynamics of three parabolic solitons with different openings. Structurally, they may achieve a process of energy concentration that does not affect each other.
- Fig. 6c displays the dynamics of the interaction of two parabolic solitons with same openings and one line-soliton.
- Fig. 6d displays the dynamics of the interaction of two parabolic solitons with opposite openings and one line-soliton. Fig. 6c and 6d describes the process of an energy beam (one line-solitons) passing through the center when condensate occurs.
- Fig. 6e shows the dynamics of the interaction of two uncrossed line-solitons and one parabolic soliton when we choose the $\mu_1 = -3,\ v_1 = 2,\ \kappa_1 = 0,\ \mu_2 = -\frac{11}{5} + 5\mathrm{i},\ \kappa_2 = 0,\ \mu_3 = -2 + 4\mathrm{i},\ \kappa_3 = 0$.
- Fig. 6f shows the dynamics of the interaction of two crossed line-solitons and one parabolic soliton we change $v_1 = 2$ to $v_1 = 1$, $\mu_2 = -\frac{11}{5} + 5\mathrm{i}$ to $\mu_2 = -\frac{11}{5} - 5\mathrm{i}$, $\mu_3 = -2 + 4\mathrm{i}$ to $\mu_3 = \frac{9}{5} + 4\mathrm{i}$ on the basic of parameters of Fig. 6e. Fig. 6e and f describes the process of two energy beams (two line-solitons) passing through the center when condensate occurs.
- Fig. 6g shows the dynamics of the weak interaction of two crossed line-solitons and one parabolic soliton when we choose the $\mu_1 = 1.8 - i, v_1 = \frac{1}{2} + \frac{\mathrm{i}}{3},\ \kappa_1 = 0,\ \mu_2 = -1.5 + 1.8\mathrm{i},\ \kappa_2 = 0,\ \mu_3 = 2 - \frac{3\mathrm{i}}{4},\ \kappa_3 = 0$ and $\alpha_0 = 1$. This shows that the linear-soliton and the parabolic soliton can also achieve independent condensation.
- Fig. 6h shows interaction of three line-solitons. The interaction of three line-solitons occurs at the center of field. After their interaction, they remain in their original state and continue to propagate until they disappear.

Remark 3. The dynamics of the interaction of three-soliton is similar to that of two-soliton, and new energy and amplitude can be obtained when they condense in the center of field. From results, we can obtain the condensate and annihilation process of the infinite soliton energy beam, theoretically.

In fact, we can also give the asymptotic forms of three-soliton, whose asymptotic expression is similar to that of two solitons, which is omitted here. Thus, we can give the abundant interaction phenomena of the three-soliton structure as a function of the analysis of one- and two-soliton. At this time, we can choose appropriate parameters to present rich soliton interaction phenomena. The multi-soliton represents the process of energy concentration from the edge into the center of the field. It also provides a reliable theoretical basis for soliton transmission, generation and interaction in experiments.

Conclusions

We have studied a two-dimensional GPE (4) in BEC in this paper. The Hirota bilinear Eq. (11) of Eq. (6) has been constructed, and by the transformation (5), the exact bright-multi-soliton solutions of Eq. (4) can be gained. Some one-, two- and three-soliton structures including parabolic soliton, dromion-like structure, and line-soliton have been exhibited in Figs. 1, 3 and 6. Fig. 2 has displayed the phase diagram for the direction of rotation or translation of parabolic-soliton with relevant parameters change. Elastic interactions of two-soliton have been analyzed through asymptotic analysis method. Figs. 4 and 5 have investigated energy changes and interaction processes of soliton. This vividly has described the process of energy gathering and annihilating in a field.

Based on the obtained soliton solutions of system (4), this paper has explored the changes in the transmission direction and energy of solitons with different bright solitons. Bright solitons have richer interactions than dark solitons. In the experiments, bright solitons have been easier to implement and have more extensive applications, and it is important to investigate the properties of bright solitons. The GPE is a very important model in physics, hence, its exact soliton solutions have also more significance. Based on the important nonlinear model in BEC, results in this paper have theoretically predicted some new nonlinear phenomena in BEC, which are helpful for us to understand some physical phenomena and physical experiments in BEC or related fields. The acquired exact solutions in this paper are new structures in this model, and it is likely that these results will be useful for the study of novel nonlinear waves that will appear in related fields in the future. For example, the results are used for simulating or understanding some nonlinear phenomena that occur during atomic condensation in BEC. The Hirota bilinear method and the asymptotic analysis of soliton are also important methods for solving soliton and analyzing them. These methods used can be applied to other important nonlinear models. These soliton solutions are also important for the study of optical signals, plasma physics, oceanophysics and biophysics. In next work, we will try to consider more complex and interesting wave function solutions when the coefficient is not constant. Moreover, the dynamical behavior of these solutions will be discussed via numerical simulation in the furture.

Compliance with Ethics Requirements

This article does not contain any studies with human or animal subjects.

Declaration of Competing Interest

The authors declare that they have no known competing financial interests or personal relationships that could have appeared to influence the work reported in this paper.

Acknowledgments

This work has been supported by the National Natural Science Foundation of China (11875008,12075034,11975172,11975001); Fundamental Research Funds for the Central Universities (2019XD-A09-3).

Appendix A. The expressions of g_3, f_2 and f_4 in two-soliton solution (15)

The parameters in two-soliton solution (15) are $g_3 = m_1 e^{\eta_1+\eta_2+\eta_1^*} + m_2 e^{\eta_1+\eta_2+\eta_2^*}$, $f_2 = n_1 e^{\eta_1+\eta_1^*} + n_2 e^{\eta_2+\eta_2^*} + n_3 e^{\eta_1+\eta_2^*} + n_4 e^{\eta_2+\eta_1^*}$ and $f_4 = n_5 e^{\eta_1+\eta_1^*+\eta_2+\eta_2^*}$, where

$$\eta_1 = \mu_1 x + v_1 y + c_1(t) + \kappa_1,$$

$$\eta_2 = \mu_2 x + v_2 y + c_2(t) + \kappa_2, c_j(t) = \frac{\mathrm{i}}{2}\left(\mu_j^2 + v_j^2\right) \int e^{2r(t)} \mathrm{d}t (j = 1, 2),$$

$$m_1 = \frac{|C_1|^2 C_2 \alpha_0 [(\mu_1 - \mu_2)^2 + (v_1 - v_2)^2]}{[(\mu_1 + \mu_1^*)^2 + (v_1 + v_1^*)^2][(\mu_2 + \mu_1^*)^2 + (v_2 + v_1^*)^2]},$$

$$m_2 = \frac{|C_2|^2 C_1 \alpha_0 [(\mu_1 - \mu_2)^2 + (v_1 - v_2)^2]}{[(\mu_2 + \mu_2^*)^2 + (v_2 + v_2^*)^2][(\mu_1 + \mu_2^*)^2 + (v_1 + v_2^*)^2]},$$

$$n_1 = \frac{|C_1|^2 \alpha_0}{(\mu_1 + \mu_1^*)^2 + (v_1 + v_1^*)^2}, n_2 = \frac{|C_2|^2 \alpha_0}{(\mu_2 + \mu_2^*)^2 + (v_2 + v_2^*)^2},$$

$$n_3 = \frac{C_1 C_2^* \alpha_0}{(\mu_1 + \mu_2^*)^2 + (v_1 + v_2^*)^2},$$

$$n_4 = \frac{C_2 C_1^* \alpha_0}{(\mu_2 + \mu_1^*)^2 + (v_2 + v_1^*)^2},$$

$$v_2 = \frac{\mu_2^{(\mathrm{R})} v_1^{(\mathrm{R})}}{\mu_1^{(\mathrm{R})}} + \mathrm{i}\frac{\mu_1^{(\mathrm{R})} v_1^{(\mathrm{I})} - v_1^{(\mathrm{R})}\mu_1^{(\mathrm{I})} + v_1^{(\mathrm{R})}\mu_2^{(\mathrm{I})}}{\mu_1^{(\mathrm{R})}},$$

$$n_5 = \frac{|C_1 C_2|^2 \alpha_0^2 [(\mu_1 - \mu_2)^2 + (v_1 - v_2)^2][(\mu_1^* - \mu_2^*)^2 + (v_1^* - v_2^*)^2]}{[(\mu_1 + \mu_1^*)^2 + (v_1 + v_1^*)^2][(\mu_2 + \mu_2^*)^2 + (v_2 + v_2^*)^2][(\mu_1 + \mu_2^*)^2 + (v_1 + v_2^*)^2][(\mu_2 + \mu_1^*)^2 + (v_2 + v_1^*)^2]},$$

the parameters u_1, u_2, v_1, κ_1 and κ_2 are any complex constants.

Appendix B. The expressions of g_3, g_5, f_2, f_4 and f_6 in two-soliton solution (18)

The parameters in three-soliton solution (18) are

$$g_3 = \sum_{j=1}^{3} m_j \mathrm{e}^{\eta_1+\eta_2+\eta_j^*} + \sum_{j=1}^{3} m_{j+3} \mathrm{e}^{\eta_1+\eta_3+\eta_j^*} + \sum_{j=1}^{3} m_{j+6} \mathrm{e}^{\eta_2+\eta_3+\eta_j^*},$$

$$g_5 = p_1 \mathrm{e}^{\eta_1+\eta_2+\eta_3+\eta_1^*+\eta_2^*} + p_2 \mathrm{e}^{\eta_1+\eta_2+\eta_3+\eta_1^*+\eta_3^*} + p_3 \mathrm{e}^{\eta_1+\eta_2+\eta_3+\eta_2^*+\eta_3^*},$$

$$f_2 = \sum_{j=1}^{3} n_j \mathrm{e}^{\eta_1+\eta_j^*} + \sum_{j=1}^{3} n_{j+3} \mathrm{e}^{\eta_2+\eta_j^*} + \sum_{j=1}^{3} n_{j+6} \mathrm{e}^{\eta_3+\eta_j^*},$$

$$\begin{aligned} f_4 = {} & q_1 \mathrm{e}^{\eta_1+\eta_2+\eta_1^*+\eta_2^*} + q_2 \mathrm{e}^{\eta_1+\eta_2+\eta_1^*+\eta_3^*} + q_3 \mathrm{e}^{\eta_1+\eta_2+\eta_2^*+\eta_3^*} \\ & + q_4 \mathrm{e}^{\eta_1+\eta_3+\eta_1^*+\eta_2^*} + q_5 \mathrm{e}^{\eta_1+\eta_3+\eta_1^*+\eta_3^*} + q_6 \mathrm{e}^{\eta_1+\eta_3+\eta_2^*+\eta_3^*} \\ & + q_7 \mathrm{e}^{\eta_2+\eta_3+\eta_1^*+\eta_2^*} + q_8 \mathrm{e}^{\eta_2+\eta_3+\eta_1^*+\eta_3^*} + q_9 \mathrm{e}^{\eta_2+\eta_3+\eta_2^*+\eta_3^*}, \end{aligned}$$

$$f_6 = l_1 \mathrm{e}^{\eta_1+\eta_2+\eta_3+\eta_1^*+\eta_2^*+\eta_3^*},$$

$$\eta_j = \mu_j x + v_j y + c_j(t) + \kappa_j, c_j = \frac{\mathrm{i}}{2}\left(\mu_j^2 + v_j^2\right) \int \mathrm{e}^{2r(t)} \mathrm{d}t,$$

$$m_j = \frac{n_j n_{j+3}[(\mu_1 - \mu_2)^2 + (v_1 - v_2)^2]}{C_j^* \alpha_0},$$

$$m_{j+3} = \frac{n_j n_{j+6}[(\mu_1 - \mu_3)^2 + (v_1 - v_3)^2]}{C_j^* \alpha_0},$$

$$m_{j+6} = \frac{n_{j+3} n_{j+6}[(\mu_2 - \mu_3)^2 + (v_2 - v_3)^2]}{C_j^* \alpha_0},$$

$$n_j = \frac{C_1 C_j^* \alpha_0}{(\mu_1 + \mu_j^*)^2 + (v_1 + v_j^*)^2},$$

$$n_{j+3} = \frac{C_2 C_j^* \alpha_0}{(\mu_2 + \mu_j^*)^2 + (v_2 + v_j^*)^2},$$

$$n_{j+6} = \frac{C_3 C_j^* \alpha_0}{(\mu_3 + \mu_j^*)^2 + (v_3 + v_j^*)^2},\ j = 1, 2, 3,$$

$$p_1 = \frac{|C_1 C_2|^2 C_3 \alpha_0^2 \rho [(\mu_1^* - \mu_2^*)^2 + (v_1^* - v_2^*)^2]}{\prod\limits_{\substack{s=1,2 \\ k=1,2,3}} [(\mu_k + \mu_s^*)^2 + (v_k + v_s^*)^2]},$$

$$p_2 = \frac{|C_1 C_3|^2 C_2 \alpha_0^2 \rho [(\mu_1^* - \mu_3^*)^2 + (v_1^* - v_3^*)^2]}{\prod\limits_{\substack{s=1,3 \\ k=1,2,3}} [(\mu_k + \mu_s^*)^2 + (v_k + v_s^*)^2]},$$

$$p_3 = \frac{|C_2 C_3|^2 C_1 \alpha_0^2 \rho [(\mu_2^* - \mu_3^*)^2 + (v_2^* - v_3^*)^2]}{\prod\limits_{\substack{s=2,3 \\ k=1,2,3}} [(\mu_k + \mu_s^*)^2 + (v_k + v_s^*)^2]},$$

$$v_2 = \frac{\mu_2^{(\mathrm{R})} v_1^{(\mathrm{R})}}{\mu_1^{(\mathrm{R})}} + \mathrm{i}\frac{\mu_1^{(\mathrm{R})} v_1^{(\mathrm{I})} - v_1^{(\mathrm{R})}\mu_1^{(\mathrm{I})} + v_1^{(\mathrm{R})}\mu_2^{(\mathrm{I})}}{\mu_1^{(\mathrm{R})}},$$

$$v_3 = \frac{\mu_3^{(\mathrm{R})} v_2^{(\mathrm{R})}}{\mu_2^{(\mathrm{R})}} + \mathrm{i}\frac{\mu_2^{(\mathrm{R})} v_2^{(\mathrm{I})} - v_2^{(\mathrm{R})}\mu_2^{(\mathrm{I})} + v_2^{(\mathrm{R})}\mu_3^{(\mathrm{I})}}{\mu_2^{(\mathrm{R})}},$$

$$\begin{aligned} \rho = {} & [(\mu_1 - \mu_2)^2 + (v_1 - v_2)^2] + [(\mu_2 - \mu_3)^2 + (v_2 - v_3)^2] \\ & + [(\mu_1 - \mu_3)^2 + (v_1 - v_3)^2], \end{aligned}$$

$$q_1 = \frac{|C_1 C_2|^2 \alpha_0^2 [(\mu_1 - \mu_2)^2 + (v_1 - v_2)^2][(\mu_1^* - \mu_2^*)^2 + (v_1^* - v_2^*)^2]}{[(\mu_1 + \mu_1^*)^2 + (v_1 + v_1^*)^2][(\mu_2 + \mu_2^*)^2 + (v_1 + v_2^*)^2][(\mu_2 + \mu_1^*)^2 + (v_2 + v_1^*)^2][(\mu_1 + \mu_2^*)^2 + (v_1 + v_2^*)^2]},$$

$$q_2 = \frac{|C_1|^2 C_2 C_3^* \alpha_0^2 [(\mu_1 - \mu_2)^2 + (v_1 - v_2)^2][(\mu_1^* - \mu_3^*)^2 + (v_1^* - v_3^*)^2]}{[(\mu_1 + \mu_1^*)^2 + (v_1 + v_1^*)^2][(\mu_2 + \mu_1^*)^2 + (v_2 + v_1^*)^2][(\mu_2 + \mu_3^*)^2 + (v_2 + v_3^*)^2][(\mu_1 + \mu_3^*)^2 + (v_1 + v_3^*)^2]},$$

$$q_3 = \frac{|C_2|^2 C_1 C_3^* \alpha_0^2 [(\mu_1 - \mu_2)^2 + (v_1 - v_2)^2][(\mu_2^* - \mu_3^*)^2 + (v_2^* - v_3^*)^2]}{[(\mu_1 + \mu_2^*)^2 + (v_1 + v_2^*)^2][(\mu_1 + \mu_3^*)^2 + (v_1 + v_3^*)^2][(\mu_2 + \mu_3^*)^2 + (v_2 + v_3^*)^2][(\mu_2 + \mu_2^*)^2 + (v_2 + v_2^*)^2]},$$

$$q_4 = \frac{|C_1|^2 C_3 C_2^* \alpha_0^2 [(\mu_1 - \mu_3)^2 + (v_1 - v_3)^2][(\mu_1^* - \mu_2^*)^2 + (v_1^* - v_2^*)^2]}{[(\mu_1 + \mu_1^*)^2 + (v_1 + v_1^*)^2][(\mu_1 + \mu_2^*)^2 + (v_1 + v_2^*)^2][(\mu_3 + \mu_2^*)^2 + (v_3 + v_2^*)^2][(\mu_3 + \mu_1^*)^2 + (v_3 + v_1^*)^2]},$$

$$q_5 = \frac{|C_1 C_3|^2 \alpha_0^2 [(\mu_1 - \mu_3)^2 + (v_1 - v_3)^2][(\mu_1^* - \mu_3^*)^2 + (v_1^* - v_3^*)^2]}{[(\mu_1 + \mu_1^*)^2 + (v_1 + v_1^*)^2][(\mu_1 + \mu_3^*)^2 + (v_1 + v_3^*)^2][(\mu_3 + \mu_3^*)^2 + (v_3 + v_3^*)^2][(\mu_3 + \mu_1^*)^2 + (v_3 + v_1^*)^2]},$$

$$q_6 = \frac{|C_3|^2 C_1 C_2^* \alpha_0^2 [(\mu_1 - \mu_3)^2 + (v_1 - v_3)^2][(\mu_2^* - \mu_3^*)^2 + (v_2^* - v_3^*)^2]}{[(\mu_1 + \mu_2^*)^2 + (v_1 + v_2^*)^2][(\mu_3 + \mu_3^*)^2 + (v_3 + v_3^*)^2][(\mu_1 + \mu_3^*)^2 + (v_1 + v_3^*)^2][(\mu_3 + \mu_2^*)^2 + (v_3 + v_2^*)^2]},$$

$$q_7 = \frac{|C_2|^2 C_3 C_1^* \alpha_0^2 [(\mu_2 - \mu_3)^2 + (v_2 - v_3)^2][(\mu_1^* - \mu_2^*)^2 + (v_1^* - v_2^*)^2]}{[(\mu_2 + \mu_1^*)^2 + (v_2 + v_1^*)^2][(\mu_3 + \mu_2^*)^2 + (v_3 + v_2^*)^2][(\mu_2 + \mu_2^*)^2 + (v_2 + v_2^*)^2][(\mu_3 + \mu_1^*)^2 + (v_3 + v_1^*)^2]},$$

$$q_8 = \frac{|C_3|^2 C_2 C_1^* \alpha_0^2 [(\mu_1^* - \mu_3^*)^2 + (v_1^* - v_3^*)^2][(\mu_2 - \mu_3)^2 + (v_2 - v_3)^2]}{[(\mu_2 + \mu_1^*)^2 + (v_2 + v_1^*)^2][(\mu_2 + \mu_3^*)^2 + (v_2 + v_3^*)^2][(\mu_3 + \mu_3^*)^2 + (v_3 + v_3^*)^2][(\mu_3 + \mu_1^*)^2 + (v_3 + v_1^*)^2]},$$

$$q_9 = \frac{|C_2 C_3|^2 \alpha_0^2 [(\mu_2^* - \mu_3^*)^2 + (v_2^* - v_3^*)^2][(\mu_2 - \mu_3)^2 + (v_2 - v_3)^2]}{[(\mu_2 + \mu_2^*)^2 + (v_2 + v_2^*)^2][(\mu_2 + \mu_3^*)^2 + (v_2 + v_3^*)^2][(\mu_3 + \mu_3^*)^2 + (v_3 + v_3^*)^2][(\mu_3 + \mu_2^*)^2 + (v_3 + v_2^*)^2]},$$

$$l_1 = \frac{\alpha_0^3 |C_1 C_2 C_3 [(\mu_1 - \mu_2)^2 + (v_1 - v_2)^2][(\mu_1 - \mu_3)^2 + (v_1 - v_3)^2][(\mu_2 - \mu_3)^2 + (v_2 - v_3)^2]|^2}{|[(\mu_1 + \mu_2^*)^2 + (v_1 + v_2^*)^2][(\mu_3 + \mu_1^*)^2 + (v_3 + v_1^*)^2][(\mu_2 + \mu_3^*)^2 + (v_2 + v_3^*)^2]|^2 \sigma},$$

$$\begin{aligned} \sigma = {} & [(\mu_1 + \mu_1^*)^2 + (v_1 + v_1^*)^2][(\mu_2 + \mu_2^*)^2 + (v_2 + v_2^*)^2][(\mu_3 + \mu_3^*)^2 \\ & + (v_3 + v_3^*)^2], \end{aligned}$$

the parameters u_j, v_j, κ_j, $j = 1, 2, 3$ are any complex constants.

References

[1] Zabusky N, Porter M. Soliton. Scholarpedia 2010;5(8):2068.
[2] Chai X, Lao D, Fujimoto K, Hamazaki R, Ueda M, Raman C. Magnetic solitons in a spin-1 Bose-Einstein condensate. Phys Rev Lett 2020;125:030402.
[3] Lannig S, Schmied C-M, Prüfer M, Kunkel P, Strohmaier R, Strobel H, et al. Collisions of three-component vector solitons in Bose-Einstein condensates. Phys Rev Lett 2020;125:170401.
[4] Wang LX, Dai CQ, Wen L, Liu T, Jiang HF, et al. Dynamics of vortices followed by the collapse of ring dark solitons in a two-component Bose-Einstein condensate. Phys Rev A 2018;97:063607.
[5] Kuznetsov EA, Rubenchik AM, Zakharov VE. Soliton stability in plasmas and hydrodynamics. Phys Rep 1986;142(3):103–65.
[6] Congy T, El G, Roberti G. Soliton gas in bidirectional dispersive hydrodynamics. Phys Rev E 2021;103:042201.
[7] Gu C, editor. Soliton Theory and Its Applications. Berlin, Heidelberg: Springer Berlin Heidelberg; 1995.
[8] Agrawal GP. Nonlinear fiber optics. fifth ed. New York: Academic Press; 2013.
[9] Wang LL, Liu WJ. Stable soliton propagation in a coupled (2+1) dimensional Ginzburg-Landau system. Chin Phys B 2020;29:070502.
[10] Yan YY, Liu WJ. Soliton rectangular pulses and bound states in a dissipative system modeled by the variable-coefficientscomplex cubic-quintic Ginzburg-Landau equation. Chin Phys Lett 2021;38:094201.
[11] Yu W, Zhou Q, Mirzazadeh M, Liu W, Biswas A. Phase shift, amplification, oscillation and attenuation of solitons in nonlinear optics. J Adv Res 2019;15:69–76.
[12] Liu X, Zhou Q, Biswas A, Alzahrani AK, Liu W. The similarities and differences of different plane solitons controlled by (3+1)-Dimensional coupled variable coefficient system. J Adv Res 2020;24:167–73.
[13] Yusuf A, Sulaiman TA. Dynamics of Lump-periodic, breather and two-wave solutions with the long wave in shallow water under gravity and 2D nonlinear lattice. Commun Nonlinear Sci Numer Simulat 2021;99:105846.
[14] Yusuf A, Sulaiman TA, Khalil EM, Bayram M, Ahmad H. Construction of multi-wave complexiton solutions of the Kadomtsev-Petviashvili equation via two efficient analyzing techniques. Res Phys 2021;21:103775.

[15] Wang HT, Wen XY. Dynamics of discrete soliton propagation and elastic interaction in a higher-order coupled Ablowitz-Ladik equation. Appl Math Lett 2020;100:106013.
[16] Wang HT, Wen XY. Soliton elastic interactions and dynamical analysis of a reduced integrable nonlinear Schrödinger system on a triangular-lattice ribbon. Nonlinear Dyn 2020;100(2):1571–87.
[17] Zhang G, Chen S, Yan Z. Focusing and defocusing Hirota equations with non-zero boundary conditions: inverse scattering transforms and soliton solutions. Commun Nonlinear Sci Numer Simulat 2020;80:104927.
[18] Kumar Barman H, Aktar MS, Uddin MH, Akbar MA, Baleanu D, Osman MS. Physically significant wave solutions to the Riemann wave equations and the Landau-Ginsburg-Higgs equation. Results Phys 2021;27:104517.
[19] Ali KK, Cattani C, Gómez-Aguilar JF, Baleanu D, Osman MS. Analytical and numerical study of the DNA dynamics arising in oscillator-chain of Peyrard-Bishop model. Chaos Soliton Fract 2020;139:110089.
[20] Chen YQ, Tang YH, Manafian J, Rezazadeh H, Osman MS. Dark wave, rogue wave and perturbation solutions of Ivancevic option pricing model. Nonlinear Dyn 2021;105(3):2539–48.
[21] Kayum MA, Roy R, Akbar MA, Osman MS. Study of W-shaped, V-shaped, and other type of surfaces of the ZK-BBM and GZD-BBM equations. Opt Quant Electron 2021;53:387.
[22] Li YM, Baskonus HM, Khudhur AM. Investigations of the complex wave patterns to the generalized Calogero-Bogoyavlenskii-Schiff equation. Soft Comput 2021;25(10):6999–7008.
[23] Khader MM, Saad KM, Hammouch Z, Baleanu D. A spectral collocation method for solving fractional KdV and KdV-Burger's equations with non-singular kernel derivatives. Appl Numer Math 2021;161:137–46.
[24] Jaradat I, Alquran M, Sivasundaram S, Baleanu D. Simulating the joint impact of temporal and spatial memory indices via a novel analytical scheme. Nonlinear Dyn 2021;103(3):2509–24.
[25] Jena RM, Chakraverty S, Baleanu D. A novel analytical technique for the solution of time-fractional Ivancevic option pricing model. Phys A 2020;550:124380.
[26] Sweilam NH, Hasan MMA. Efficient method for fractional Lévy-Feller advection-dispersion equation using Jacobi polynomials. Progr. Fract. Differ. Appl. 2020;6:115–28.
[27] Gross EP. Hydrodynamics of a superfluid condensate. J Math Phys 1963;4 (2):195–207.
[28] Pitaevskii LP. Vortex lines in an imperfect Bose gas. Sov. Phys. JETP 1961;13:451.
[29] Sulem C, Sulem PL. The Nonlinear Schrödinger Equation. Berlin Heidelberg: Springer; 1999.
[30] Kevrekidis PG, Frantzeskakis DJ, Carretero-González R, et al., editors. Emergent Nonlinear Phenomena in Bose-Einstein Condensates. Berlin, Heidelberg: Springer Berlin Heidelberg; 2008.
[31] Anderson MH, Ensher JR, Matthews MR, Wieman CE, Cornell EA. Observation of Bose-Einstein condensation in a dilute atomic vapor. Science 1995;269 (5221):198–201.
[32] Davis KB, Mewes M-O, Andrews MR, van Druten NJ, Durfee DS, Kurn DM, et al. Bose-Einstein condensation in a gas of sodium atoms. Phys Rev Lett 1995;75 (22):3969–73.
[33] Bradley CC, Sackett CA, Tollett JJ, Hulet RG. Evidence of Bose-Einstein condensation in an atomic gas with attractive interactions. Phys Rev Lett 1995;75(9):1687–90.
[34] Cornish SL, Thompson ST, Wieman CE. Formation of bright matter-wave solitons during the collapse of attractive Bose-Einstein condensates. Phys Rev Lett 2006;96:170401.
[35] Strecker KE, Partridge GB, Truscott AG, Hulet RG. Formation and propagation of matter-wave soliton trains. Nature 2002;417(6885):150–3.
[36] Khaykovich L, Schreck F, Ferrari G, Bourdel T, Cubizolles J, et al. Formation of a matter-wave bright soliton. Science 2002;296:1290.
[37] Denschlag J, Simsarian JE, Feder DL, Clark CW, et al. Generating solitons by phase engineering of a Bose-Einstein condensate. Science 2000;287:97–101.
[38] Burger S, Bongs K, Dettmer S, Ertmer W, Sengstock K, Sanpera A, et al. Dark solitons in Bose-Einstein condensates. Phys Rev Lett 1999;83(25):5198–201.
[39] Hu XH, Zhang XF, Zhan D, Luo HG, Liu WM. Dynamics and modulation of ring dark solitons in two-dimensional Bose-Einstein condensates with tunable interaction. Phys Rev A 2009;79:023619.
[40] Wu XY, Tian B, Qu QX, Yuan YQ, Du XX. Rogue waves for a (2+1)-dimensional Gross-Pitaevskii equation with time-varying trapping potential in the Bose-Einstein condensate. Comput Math Appl 2020;79:1023–30.
[41] Guo H, Wang YJ, Wang LX, Zhang XF. Dynamics of ring dark solitons in Bose-Einstein condensates. Acta Phys Sin 2020;69:010302.
[42] Yu F. Inverse scattering solutions and dynamics for a nonlocal nonlinear Gross-Pitaevskii equation with PT-symmetric external potentials. Appl Math Lett 2019;92:108–14.
[43] Su CQ, Gao YT, Xue L, Wang QM. Nonautonomous solitons, breathers and rogue waves for the Gross-Pitaevskii equation in the Bose-Einstein condensate. Commun Nonlinear Sci Numer Simulat 2016;36:457–67.
[44] Xu T, Chen Y. Darboux transformation of the coupled nonisospectral Gross-Pitaevskii system and its multi-component generalization. Commun Nonlinear Sci Numer Simulat 2018;57:276–89.
[45] Alotaibi MOD, Carr LD. Internal oscillations of a dark-bright soliton in a harmonic potential. J Phys B: At Mol Opt Phys 2018;51:205004.
[46] Dai CQ, Wang XG, Zhou GQ. Stable light-bullet solutions in the harmonic and parity-time-symmetric potentials. Phys Rev A 2014;89:013834.
[47] Yuan YQ, Tian B, Qu QX, Zhang CR, Du XX. Lax pair, binary Darboux transformation and dark solitons for the three-component Gross-Pitaevskii system in the spinor Bose-Einstein condensate. Nonlinear Dyn 2020;99 (4):3001–11.
[48] Caputo M, Fabrizio M. On the singular kernels for fractional derivatives. Some applications to partial differential equations. Progr Fract Differ Appl 2021;7:79–82.
[49] Saito Hiroki, Ueda Masahito. Dynamically stabilized bright solitons in a two-dimensional Bose-Einstein condensate. Phys Rev Lett 2003;90:040403.
[50] Hirota Ryogo. Exact solution of the Korteweg-de Vries equation for multiple collisions of solitons. Phys Rev Lett 1971;27(18):1192–4.
[51] Hietarinta J. Introduction to the Hirota bilinear method; 1997. arXiv:solv-int/9708006v1.
[52] Qiao Z, Li X. An integrable equation with nonsmooth solitons. Theor Math Phys 2011;167:584–9.
[53] Zhang HQ, Tian B, Lü X, Li H, Meng XH. Soliton interaction in the coupled mixed derivative nonlinear Schrödinger equations. Phys Lett A 2009;373:4315–21.
[54] Xu T, Tian B, Li LL, Lü X, Zhang C. Dynamics of Alfvén solitons in inhomogeneous plasmas. Phys Plasmas 2008;15(10):102307.